

Nanomaterial-Modified Capacitive Field-Effect Biosensors



Arshak Poghossian and Michael J. Schöning

Abstract The coupling of charged molecules, nanoparticles, and more generally, inorganic/organic nanohybrids with semiconductor field-effect devices based on an electrolyte–insulator–semiconductor (EIS) system represents a very promising strategy for the active tuning of electrochemical properties of these devices and, thus, opening new opportunities for label-free biosensing by the intrinsic charge of molecules. The simplest field-effect sensor is a capacitive EIS sensor, which represents a (bio-)chemically sensitive capacitor. In this chapter, selected examples of recent developments in the field of label-free biosensing using nanomaterial-modified capacitive EIS sensors are summarized. In the first part, we present applications of EIS sensors modified with negatively charged gold nanoparticles for the label-free electrostatic detection of positively charged small proteins and macromolecules, for monitoring the layer-by-layer formation of oppositely charged polyelectrolyte (PE) multilayers as well as for the development of an enzyme-based biomolecular logic gate. In the second part, examples of a label-free detection by means of EIS sensors modified with a positively charged weak PE layer are demonstrated. These include electrical detection of on-chip and in-solution hybridized DNA (deoxyribonucleic acid) as well as an EIS sensor with pH-responsive weak PE/enzyme multilayers for enhanced field-effect biosensing.

Keywords Biomolecular logic gate, DNA, Enzyme biosensor, Field-effect sensor, Gold nanoparticle, Polyelectrolyte

A. Poghossian (✉) and M. J. Schöning (✉)
Institute of Nano- and Biotechnologies, FH Aachen, Campus Jülich Heinrich-Mußmannstr. 1,
52428 Jülich, Germany
e-mail: a.poghossian@fz-juelich.de; schoening@fh-aachen.de

M. J. Schöning, A. Poghossian (eds.), *Label-Free Biosensing: Advanced Materials, Devices and Applications*, Springer Series on Chemical Sensors and Biosensors (2018) 16: 1–26
DOI 10.1007/5346_2017_2, © Springer International Publishing AG 2017,
Published online: 17 May 2017

Contents

1	Introduction	2
2	Capacitive EIS Sensors Modified with AuNP/Molecule Hybrids	3
2.1	Preparation of AuNP-Modified EIS Sensors and Measurement Setup	4
2.2	Functioning of EIS Sensors Modified with AuNP/Molecule Hybrids	6
2.3	Detection of Cytochrome c	8
2.4	Detection of Poly-D-lysine	9
2.5	Detection of LbL Adsorption of Oppositely Charged PE Macromolecules and Multilayer Formation	9
2.6	Enzyme Logic Gates Based on an AuNP-Modified EIS Sensor	11
3	Polyelectrolyte-Modified EIS Sensors	14
3.1	Label-Free Detection of DNA with PAH-Modified EIS Sensor	14
3.2	Biosensors Based on an EIS Sensor Modified with a PAH/Enzyme Multilayer	17
4	Summary and Outlook	19
	References	20

1 Introduction

The construction of nanoscale electronic devices utilizing single molecules and nanoobjects (e.g., metal, oxide and semiconductor nanoparticles, carbon nanotubes, etc.) as building blocks represents an exciting and promising approach to realize future electronics beyond the current semiconductor technologies, as electronic devices are becoming progressively smaller and silicon technology is reaching its limit. In the past decade, a number of nanoelectronic and molecular devices (e.g., single-electron transistors [1, 2], molecular transistors [3, 4]) have been proposed, which are based on unique properties of individual molecules or nanoobjects as well as new physical phenomena in the nano-world. In spite of enormous efforts devoted in the research field of molecular electronic devices, nevertheless, the replacement of Si with “molecule-only” or “nanoobject-only” technologies in the near future is considered to be a challenging task [5]. It has been widely discussed that an integration of nanoobject/biomolecule inorganic/organic functional hybrid systems with a macroscopic electronic transducer (hybrid device concept) might be a more realistic approach for a new generation of (bio-)chemical sensors, sensor arrays, and multifunctional biochips. The combination of nano- and biomaterials within a hybrid system allows an enhancement of their functional properties and often leads to new synergistic effects originating from the components of the hybrid system [6–8].

In this context, the coupling of charged molecules, nanoobjects, and inorganic/organic nanohybrids with semiconductor field-effect devices (FEDs) based on an electrolyte–insulator–semiconductor (EIS) system represents a very promising strategy for the active tuning of electrochemical properties of FEDs and, therefore, can open new opportunities for label-free biosensing with direct electrical readout [5, 9–11]. Currently, FEDs based on an EIS system represent one of the key structural elements for chemical and biological sensing (see, e.g., reviews

[12–18]). Ion-sensitive field-effect transistors (ISFET), capacitive EIS sensors, light-addressable potentiometric sensors (LAPS), and silicon nanowire transistors (SiNW) are typical examples of (bio-)chemically sensitive FEDs. These devices provide a lot of potential advantages such as small size and weight, fast response time, compatibility with advanced micro- and nanofabrication technology, the possibility of on-chip integration of multiple sensors (arrays), and signal processing circuits.

The capacitive EIS sensor is the simplest field-effect sensor and represents a (bio-)chemically sensitive capacitor. Since field-effect EIS sensors are charge-sensitive devices, in principle, they are able to detect any kind of charge (or potential) changes at or nearby the gate insulator–electrolyte interface induced by (bio-)chemical reactions or molecular interactions, in particular, adsorption and binding of molecules. In previous experiments, EIS sensors have been applied for the measurement of various (bio-)chemical quantities in liquids, like pH value, ion and analyte concentrations [19–22]. In addition, during the last few years, label-free sensing of charged molecules and nanoobjects (e.g., nanoparticles, carbon nanotubes) has become one of the most reported applications for capacitive EIS sensors [5, 11, 23–26]. The present chapter summarizes selected examples of recent developments and current research activities in the field of label-free biosensing using nanomaterial-modified capacitive field-effect sensors. These include:

1. EIS sensors modified with negatively charged gold nanoparticles (AuNP) for the label-free electrostatic detection of positively charged small proteins and macromolecules, for monitoring the layer-by-layer (LbL) formation of oppositely charged polyelectrolyte (PE) multilayers, as well as for the development of an enzyme-based molecular logic gate
2. EIS sensors modified with (a) positively charged weak PE layer for the label-free electrical detection of DNA (deoxyribonucleic acid) immobilization and hybridization by its intrinsic molecular charge and (b) weak PE/enzyme multilayer for enhanced field-effect biosensing

2 Capacitive EIS Sensors Modified with AuNP/Molecule Hybrids

Assemblies of AuNPs on a macroscopic transducer surface are an emerging and highly attractive class of chemically and electrically tunable functional materials. Due to the unique electrical, electrochemical, catalytic, and optical properties of AuNPs, different from those of bulk Au, they have been extensively applied in both fundamental research (e.g., catalysis, adsorption and binding of molecules, biotechnology, electron transport phenomena in nanoscale materials with 1D, 2D, or 3D dimensionalities) [27–29] and various application-oriented fields (optical and electronic devices, chemical sensors and biosensors, molecular logic gates, drug delivery systems, etc.) [1, 2, 5–7, 20, 30–36].

Since the surface of AuNPs can be easily modified with variously charged shell molecules and because the vast majority of biomolecules or PE macromolecules are charged under physiological conditions, AuNP-modified EIS sensors can provide a universal and efficient platform for label-free electrical detection of a wide variety of molecules by their intrinsic molecular charge. The EIS sensor detects the charge changes in those AuNP/molecule inorganic/organic hybrids induced by the molecular adsorption or binding events. Below, the feasibility of this approach is demonstrated on the examples of AuNP-modified capacitive EIS sensors for the electrostatic detection of positively charged cytochrome c (CytC) and poly-D-lysine (PDL) molecules as well as the formation of PE multilayers consisting of poly(allylamine hydrochloride) (PAH)/poly(sodium 4-styrenesulfonate) (PSS) system, representing typical model examples of detecting small proteins and macromolecules and the consecutive adsorption of positively/negatively charged PE molecules, respectively. In addition, the results of interfacing of an enzyme-based **AND–Reset** logic gate (that mimics the operation of electronic logic gates) with such EIS sensor functionalized with pH-responsive AuNPs are presented.

2.1 Preparation of AuNP-Modified EIS Sensors and Measurement Setup

The EIS sensors consisting of an Al–p-Si–SiO₂ structure (30 nm thermally grown SiO₂; 300 nm Al as rear-side contact layer) with chip sizes of 10 mm × 10 mm were prepared from a p-Si wafer (specific resistivity, 5–10 Ω cm). Before deposition of AuNPs, the SiO₂ surface was silanized with 3-mercaptopropyl trimethoxysilane (MPTMS). It is a bifunctional molecule that contains both thiol and silane functional groups and serves as a coupling agent between the AuNPs and SiO₂ [37]. The negatively charged citrate-capped AuNPs were prepared from a water solution using the well-established chloroauric acid (HAuCl₄) reduction method [38, 39]. For deposition of AuNPs on the MPTMS-modified SiO₂ surface, the sensor was immersed in a water solution of citrate-stabilized AuNPs for 12 h. The surface of the AuNP-modified EIS sensors was characterized by scanning electron microscopy (SEM) and atomic force microscopy (AFM) (see Fig. 1). The average diameter and density of AuNPs evaluated from several SEM images were approximately 18 ± 2 nm and $N = (0.8–1.2) \times 10^{11}$ AuNPs/cm², respectively. The negatively charged citrate surface provides a convenient scaffold to attach positively charged molecules. For details of surface silanization, AuNP preparation, and deposition steps, see [5].

The capacitance–voltage (*C–V*) and constant–capacitance (ConCap) modes are the most convenient methods for the electrochemical characterization of capacitive field-effect sensors [40]. The *C–V* and ConCap curves were recorded before and after surface modification or molecular adsorption process using an impedance analyzer (see Fig. 2a). In the ConCap mode, the capacitance of the EIS sensor at the

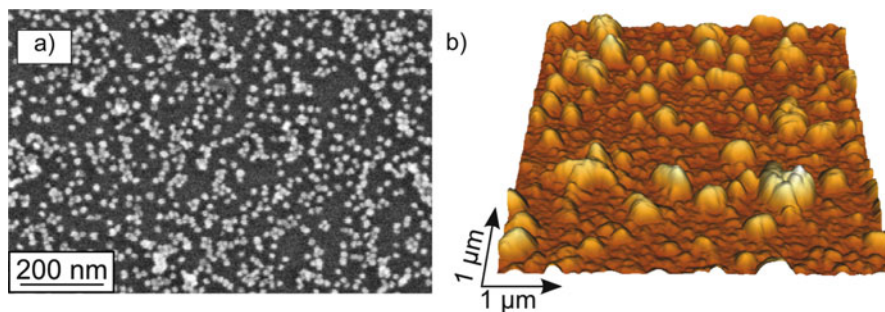


Fig. 1 SEM (a) and tapping-mode AFM (b) images of an AuNP-modified EIS sensor surface. Reproduced from [5] with permission of the Royal Society of Chemistry

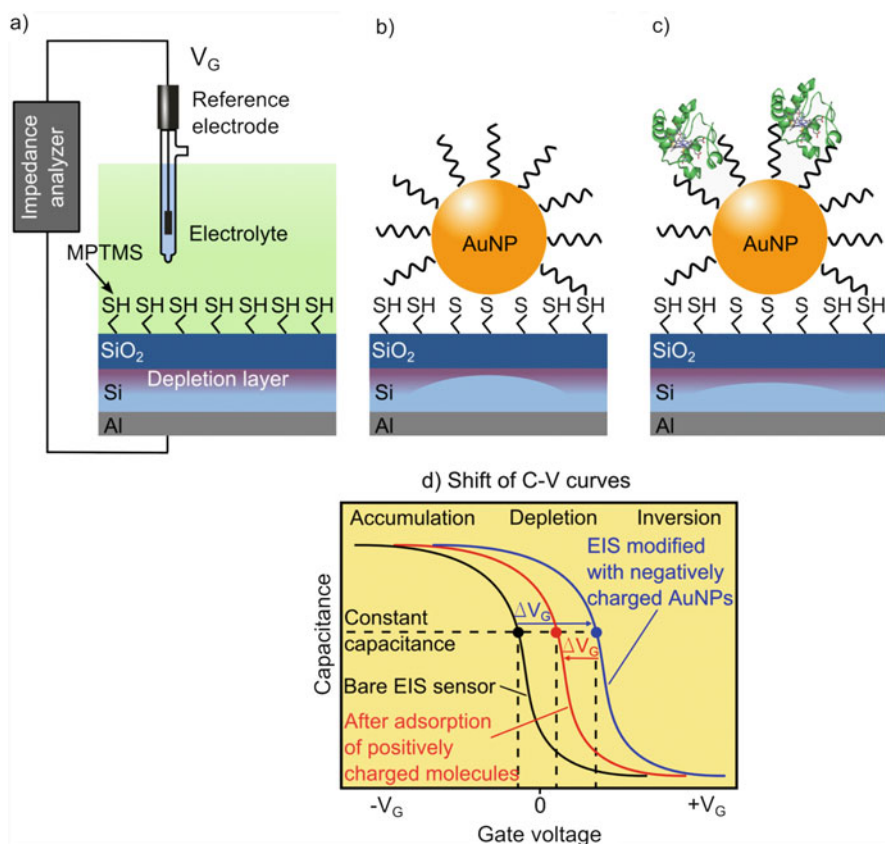


Fig. 2 Schematic cross section of the capacitive field-effect Al-p-Si-SiO₂ EIS sensor after silanization (a), deposition of negatively charged citrate-capped AuNPs (b), adsorption of positively charged molecules on the AuNPs (c), and the corresponding C-V curves with typical accumulation, depletion, and inversion regions (d). Local changes in the width of the depletion layer are shown, too. Reproduced from [5] with permission of the Royal Society of Chemistry

working point (which is usually chosen within the linear range of the depletion region of the C - V curve) is kept constant by using a feedback control circuit, and potential changes at the gate surface, induced by the molecular adsorption or binding event, are recorded directly. For operation, a DC (direct current) polarization voltage is applied to the gate via the reference electrode (conventional Ag/AgCl liquid-junction electrode) to set the working point and a small superimposed AC (alternating current) voltage (20 mV) with a frequency of 100 Hz is applied to the system to measure the capacitance of the sensor. The contact area of the EIS sensor with the solution was about 0.4 cm². All potential values are referred to the reference electrode.

2.2 *Functioning of EIS Sensors Modified with AuNP/Molecule Hybrids*

Figure 2 schematically shows the simplified measurement setup and cross section of the capacitive Al-p-Si-SiO₂ sensor structure after silanization of the SiO₂ surface (a), deposition of negatively charged citrate-capped AuNPs (b), adsorption of positively charged molecules on the AuNPs (c), and the expected shift of a high-frequency C - V curve of the bare EIS sensor after these surface modification steps (d).

In such a device, the ligand-stabilized AuNPs have a dual role: they provide a simple way for the attachment/binding of a wide variety of charged biomolecules on their surface; at the same time, AuNPs act as additional quasi-spherical metal gates, whose potential can be tuned by the intrinsic charge of attached molecules, resulting in local changes in the width of the depletion layer, as shown in Fig. 2b, c. In a simplified electrical equivalent circuit model, the total capacitance of the EIS structure, C , is usually represented as a series connection of the insulator capacitance (C_i), and the variable capacitance of the space-charge or depletion region in the semiconductor (C_{sc}) (the electrochemical double-layer capacitance is assumed to be much greater than C_i and C_{sc} and can, thus, be neglected) [40, 41]:

$$C = \frac{C_i C_{sc}}{C_i + C_{sc}} = \frac{C_i}{1 + C_i/C_{sc}} \quad (1)$$

In Eq. (1), for a given insulator thickness, the value of C_i is constant, while C_{sc} is determined by the width of the space-charge region in the semiconductor, which depends, among others, on the voltage applied to the gate, V_G , and the potential at the gate insulator/electrolyte interface. Dependent on the magnitude and polarity of the applied gate voltage, V_G , three regions in the C - V curve can be distinguished: accumulation, depletion, and inversion. In the accumulation region, $C_i \ll C_{sc}$, the total capacitance of the EIS structure is determined by the geometrical capacitance of the insulator, $C = C_i$, and corresponds to the maximum capacitance of the system (Fig. 2d).

The binding of charged species to the AuNPs is analogous to the effect of applying an additional voltage to the gate. Therefore, for the investigation of charge effects induced in a capacitive EIS structure by the adsorption or binding of charged molecules or nanoobjects, more important is the shift of the C - V curves along the voltage axis (ΔV_G) in the depletion region. The direction of these potential shifts depends on the sign of the charge of adsorbed molecules. The binding of negatively charged citrate-capped AuNPs to the silanized SiO_2 surface will decrease the width of the depletion layer (Fig. 2b) and increase the depletion capacitance (C_{sc}) in the Si within regions under surface areas covered with AuNPs. This will result in an increase of the total capacitance of the sensor and in a shift of the C - V curve in the direction of more positive (or less negative) gate voltages. In contrast, the electrostatic adsorption or binding of positively charged molecules to the negatively charged citrate-capped AuNPs will modulate the charge of the AuNP/molecule hybrids and, thus, will lead to a local increase of the width of the depletion layer (Fig. 2c) and decrease of the space-charge capacitance. As a consequence, the total capacitance of the modified EIS sensor will also decrease, resulting in a shift of the C - V curve in the direction of more negative (or less positive) gate voltages (see Fig. 2d). The amplitude of potential shifts (ΔV_G) depends on the surface coverage of the AuNPs, number of attached molecules, and their intrinsic charge and is given by [5]

$$\Delta V_G = \frac{nN_{\text{NP}}N_M Q_M}{C_d} \quad (2)$$

where N_{NP} is the surface density of the citrate-capped AuNPs, n is the AuNP-coated fraction (coverage) of the gate surface, N_M is the number of adsorbed molecules per AuNP, Q_M is the effective charge of the adsorbed molecule, and C_d is the double-layer capacitance.

Equation (2) is obtained by assuming that (a) the surface potential can be considered as the average mixed potential of the silanized SiO_2 /solution and AuNP hybrid/solution interfaces; (b) the double-layer capacitance, C_d , is similar at the AuNP hybrid/solution and silanized SiO_2 /solution interface; and (c) screening of the charge of AuNP hybrids by counterions in the solution can be neglected. It is worth noting that due to the counterion-screening effect, the effective charge of molecules and, therefore, the potential shift will depend on the ionic strength of the measurement solution. Equation (2) clearly indicates the possibility of gating field-effect EIS sensors by the charge of nanoparticle/molecule hybrids. In addition, it allows to estimate potential changes induced by the adsorption or binding of charged molecules onto AuNP-modified sensor surfaces. The large sensor signal can be expected by a high surface coverage of AuNPs, a large number of highly charged, adsorbed molecules per AuNP, and by measurements in low ionic strength solutions (i.e., by a reduced counterion-screening effect and a small double-layer capacitance).

2.3 Detection of Cytochrome *c*

CytC is an essential component of the electron transport chain in mitochondria. It is a small, nearly spherical protein with a size of $2.6 \text{ nm} \times 3.2 \text{ nm} \times 3.0 \text{ nm}$ [42]. Since the isoelectric point of CytC is around pH 10 [43], it is sufficiently positively charged at neutral pH value; the net positive charge of CytC in pH 7 solution is approximately $+9e$ (e is the elementary charge, $1.6 \times 10^{-19} \text{ C}$) [44]. CytC rapidly binds to an AuNP due to electrostatic interactions between the positively charged CytC and negatively charged citrate-capped AuNP. Figure 3 shows an example of the label-free electrical detection of CytC molecules by means of the EIS sensor modified with citrate-capped AuNPs. As can be seen, after the CytC adsorption, a large shift of the $C-V$ curve of about 328 mV in the direction to more negative voltages has been observed in the depletion region that can be attributed to the presence of positively charged CytC molecules on/close to the negatively charged citrate-capped AuNPs. Both the direction and amplitude of potential shifts can directly be determined from the dynamic ConCap-mode measurements. The number of adsorbed CytC molecules per AuNP calculated from Eq. (2) using the experimentally observed potential change of $\Delta V_G = 330 \text{ mV}$ (evaluated from the ConCap curve in Fig. 3) amounted to be approximately $N_M = 46$ [5].

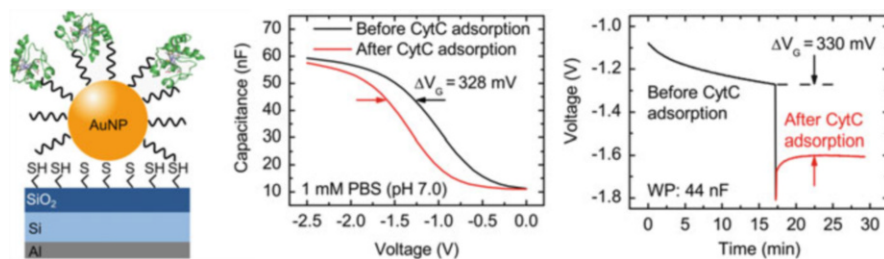


Fig. 3 Label-free electrical detection of positively charged CytC molecules by means of the EIS sensor modified with negatively charged citrate-capped AuNPs (*left*). The $C-V$ curves (*middle*) and the ConCap response (*right*) were recorded in 1 mM phosphate buffer solution (PBS) of pH 7 before and after the adsorption of CytC molecules. For the CytC adsorption, the sensor was exposed to 1 mM PBS (pH 7) containing $50 \mu\text{M}$ CytC for 10 min. The $C-V$ curves exhibit a typical high-frequency shape with the usual accumulation ($V_G < -2 \text{ V}$), depletion ($-1.7 \text{ V} < V_G < -0.75 \text{ V}$), and inversion ($V_G > -0.6 \text{ V}$) regions. *WP*: working point. Reproduced from [5] with permission of the Royal Society of Chemistry

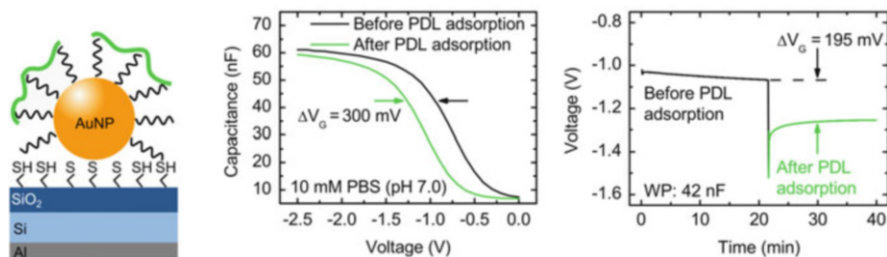


Fig. 4 Label-free detection of PDL molecules by means of a capacitive EIS sensor modified with citrate-capped AuNPs (*left*). The C - V curves (*middle*) and the ConCap response (*right*) of the EIS sensors were recorded before and after adsorption of positively charged PDL molecules. For PDL adsorption, the AuNP-modified EIS sensor was exposed to 10 mM PBS, pH 7, containing 10 mg/mL PDL for 15 min. Reproduced from [5] with permission of the Royal Society of Chemistry

2.4 Detection of Poly-D-lysine

A sketch of the EIS sensor modified with AuNP/PDL hybrids is depicted in Fig. 4 (*left*). PDL is a synthetic amino acid chain that is positively charged and widely used as a coating to enhance cell attachment and adhesion to surfaces. In weakly acidic to weakly alkaline solutions (pH 5–9), a strong electrostatic interaction exists between polycationic chains of PDL and citrate-capped AuNPs, which is a result of direct coupling of positive NH_3^+ groups of PDL with negative COO^- groups of the citrate-capped AuNPs [45, 46]. The single AuNP can serve as docking site for multiple PDL chain adsorptions. On the other hand, the PDL macromolecule can bind to multiple AuNPs.

An example for label-free electrical detection of PDL with the AuNP-modified EIS sensor is demonstrated in Fig. 4. The potential shifts detected after the adsorption of PDL molecules evaluated from the C - V curves and the ConCap response of three sensors were between 195 and 300 mV.

2.5 Detection of LbL Adsorption of Oppositely Charged PE Macromolecules and Multilayer Formation

Polyelectrolytes are macromolecules carrying a large number of charged or chargeable groups when dissolved in solution. LbL deposition of PE multilayers from solutions provides a simple, low-cost, and efficient method for the preparation of ultrathin films as well as complex heterostructures with a well-defined composition and multiple functionalities, whereby ultrathin films are assembled electrostatically from the repetitive, sequential adsorption of polyions with alternating charge [47, 48].

Recent experiments on the detection of PE macromolecules using capacitive EIS sensors [40, 49, 50], silicon thin-film resistors [51], field-effect transistors [52],

nanowire transistors [53], and metal–insulator–semiconductor devices [54] as transducer have demonstrated that the semiconductor field-effect platform represents a powerful tool for real-time, in-situ electrical monitoring of PE multilayer formation. The feasibility of an AuNP-modified capacitive EIS sensor for the label-free detection of consecutive adsorption of polyelectrolytes has recently been demonstrated using cationic weak PE PAH and anionic strong PE PSS as a model system [5].

Figure 5 presents a schematic of the LbL formation of PAH/PSS multilayers on the surface of AuNPs (a) as well as zoomed $C-V$ curves in the depletion region and a ConCap response of the AuNP-modified EIS sensor after the consecutive adsorption of each cationic PAH and anionic PSS layer from the respective PE solution (50 μM PAH or PSS, adjusted with 100 mM NaCl, pH 5.4) (b). At this pH value, both the PSS and the PAH molecules are fully charged [55]. As the citrate-capped AuNPs are negatively charged, the PE multilayer formation was started with the positively charged PAH macromolecules.

The consecutive adsorption of oppositely charged PE layers leads to alternating shifts of the $C-V$ curve and ConCap signal of the AuNP-modified EIS sensor along

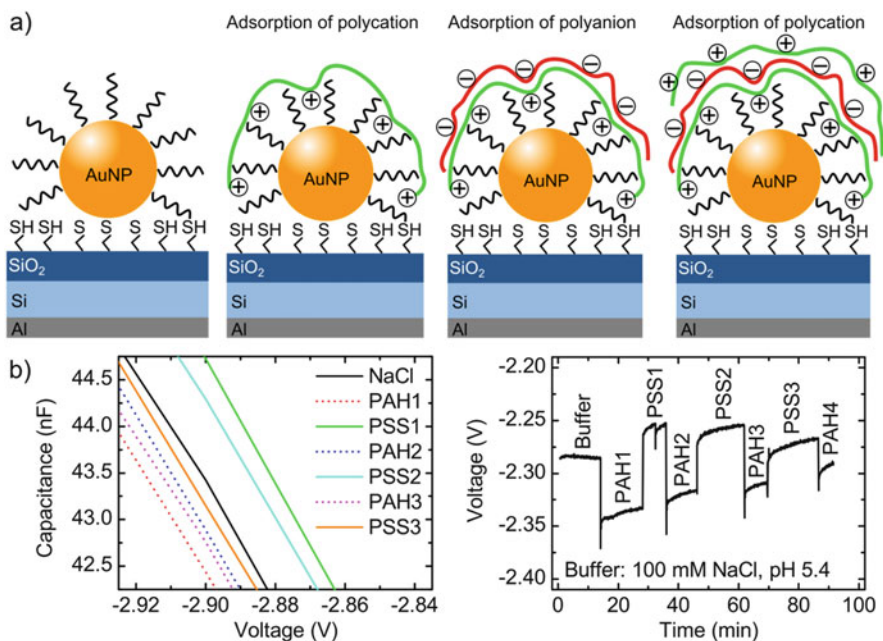


Fig. 5 Schematic of LbL formation of PAH/PSS multilayer on a surface of AuNPs (a) as well as zoomed $C-V$ curves in the depletion region (*left*) and ConCap response (*right*) of the AuNP-modified EIS sensor after the consecutive adsorption of cationic PAH and anionic PSS macromolecules (b). In this experiment, the EIS sensor was consecutively exposed to the respective PE solution for about 10 min (the time necessary for depositing a single monolayer), followed by recording of the $C-V$ curve and ConCap response. These procedures were repeated until the desired number of layers was achieved (in this study, 6–7 layers). Reproduced from [5] with permission of the Royal Society of Chemistry

the voltage axis. The direction of the signal changes correlates with the charge sign of the outermost PE layer that is in good agreement with previous studies on PE detection with various types of field-effect devices [40, 49–51, 53]. It is assumed that the charge of the outermost layer overcompensates the charge of the underlying layer and, thus, enables the adsorption of the next layer. Due to the reversal of the charge of the outermost layer, the potential shifts show a “zigzag”-like behavior. When the multilayer is terminated with the PAH layer, the sensor signal shifts toward the direction corresponding to a more positively charged gate surface. In contrast, the adsorption of a negatively charged PSS layer shifts the sensor signal to less negative gate voltages.

As can be seen from the ConCap response in Fig. 5b, the magnitude of potential shifts has a tendency to decrease with increasing the number of adsorbed PE layers. For example, the ConCap signal decreases from ~ 80 to ~ 40 mV after the formation of the first and third bilayers of PAH/PSS, respectively. A similar effect was observed for field-effect thin-film resistors and capacitive EIS sensors without AuNPs [40, 51]. To explain the impact of the number of adsorbed PE layers on the signal behavior of the capacitive EIS sensor, a simplified theoretical model that describes, among others, the influence of the distance of the outermost PE layer from the gate surface has been developed in [40]. The electrostatic coupling between the PE charge and the gate surface will drop with increasing the distance between the outermost PE layer and the sensor surface. As a consequence, the potential changes at the gate surface induced upon the PE adsorption will decrease with increasing the number of PE layers and thickness of multilayer that, in fact, has been observed in the experiment.

2.6 *Enzyme Logic Gates Based on an AuNP-Modified EIS Sensor*

The idea creating a biocomputer using different biomolecules (e.g., proteins, DNA, or enzymes) has attracted significant interest. Therefore, in the past decade, a large variety of biochemical Boolean logic gates (**AND**, **NAND**, **OR**, **XOR**, **NOR**, **INHIB**, etc.) and some more complex devices have been realized (see e.g., recent reviews [56–61]). However, most of developments on molecular logic gates and circuits represent elegant proof-of-concept experiments mimicking the operation of their electronic analogues but are not able to compete with electronic computers [57, 59, 60]. It is widely discussed that future of molecular logic elements is strongly connected with the successful transfer of biomolecular logic principles to solid substrates and integration with an electronic transducer as well as with the possibility of their addressing and switching on/off externally [57, 62]. A coupling of biomolecular logic systems with electronic transducers and stimuli-responsive materials might enable the creation of novel digital biosensors with qualitative binary output signals in a YES/NO format, logically triggered actuators for

substance- or drug-release systems [57, 59, 63–65] and even closed-loop intelligent sense/act/treat systems [66], opening a new research avenue in advanced personalized medicine and theranostics.

In this context, an integration of biomolecular logic gates with field-effect devices based on an EIS system – an electrochemical analog of the basic element of conventional electronic logic gates and computing – is considered as one of the most attractive and promising approaches for the transformation of molecular logic outputs into electrical signals. The feasibility of this approach has recently been demonstrated by realizing enzyme-based **AND–Reset** and **OR–Reset** gates using capacitive field-effect EIS sensors consisting of an Al–p–Si–SiO₂ structure functionalized with AuNPs [35] and an Al–p–Si–SiO₂–Ta₂O₅ structure modified with a multienzyme membrane [62, 67], where analytes were used as chemical input. In the following, the functioning of a field-effect-based enzyme logic gate is explained in case of an **AND–Reset** logic gate interfaced with an Al–p–Si–SiO₂ EIS sensor modified with pH-responsive AuNPs, which have thiolated shell molecules containing carboxylic groups [35]. In aqueous solution, carboxylic groups deprotonate to carboxylate anions (COO[−]), yielding in AuNPs with a negatively charged shell. In contrast to [35, 62, 67], the enzymes have been used as biochemical input signal.

Before the logic gate experiments, the pH sensitivity of the bare and AuNP-modified EIS sensors has been proven in standard buffer solutions from pH 4 to pH 9. The EIS sensors with a SiO₂ gate insulator showed a pH sensitivity of about 38–42 mV/pH that is in good accordance to values typically reported for a SiO₂ layer [68]. A slightly higher pH sensitivity of 46 mV/pH was found for EIS sensors modified with AuNPs.

The schematic of the **AND–Reset** logic gate is shown in Fig. 6a. It consists of three enzymes, glucose oxidase (GOD), invertase, and urease, added into the solution containing sucrose and dissolved oxygen. The absence of the respective enzymes is considered as the input signal **0**, while addition of enzymes is used as the input signal **1**. The operation of the enzyme logic gates is based on the cascade of enzymatic reactions. The **AND** gate was activated by invertase and GOD, while urease was used to realize the **Reset** function. The hydrolytic conversion of sucrose to glucose and fructose catalyzed by invertase was followed by glucose oxidation catalyzed by GOD in the presence of dissolved O₂. Final product of these biochemical reactions is gluconic acid, thus lowering the pH value of the solution. As a result of the pH-induced charge changes associated with the protonation/deprotonation of both the carboxylic groups of pH-responsive shells on the immobilized AuNPs and the silanol groups on the SiO₂ surface areas not covered with AuNPs, the EIS sensor generates an electronic signal (changes in the capacitance of the depletion layer in the semiconductor) corresponding to the logic output produced by the enzymes. The logic output signal has been read out by means of the C–V method. As can be seen from Fig. 6b, only if both enzymes (invertase and GOD) are present in the solution (input **1,1**), the cascade of enzymatic reactions is completed, resulting in a pH decrease and a large shift (about 118 mV) of the C–V curve toward more negative voltage values. The reaction cascade cannot start if

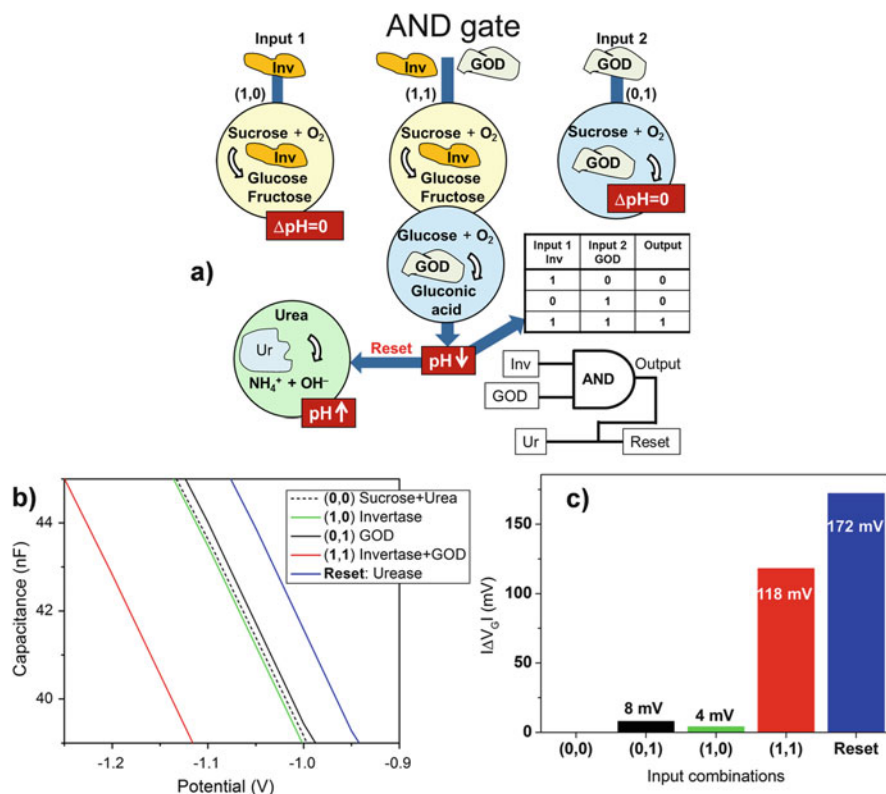


Fig. 6 Schematic of the **AND-Reset** logic gate (a), zoomed $C-V$ curves in the depletion region for the AuNP-modified EIS sensor recorded by **AND** and **Reset** operations (b), and corresponding potential shifts induced by different chemical input combinations (0,0, 1,0, 0,1, or 1,1) (c). *Inv* invertase, *Ur* urease

invertase is missing (input signal 1,0) or it cannot be completed if GOD is missing (input signal 0,1). The potential shifts by different chemical input combinations are depicted in Fig. 6c.

In order to provide the reversible operation of the **AND** gate, the pH value should be increased again [67]. This has been achieved via activation of the **Reset** function by adding the enzyme urease in the solution containing urea (10 mM). This results in a pH increase and a rapid change in the sensor signal for about 172 mV in the direction of less negative voltage values.

These experiments demonstrate an example of the successful interfacing of enzyme logic principles with the field-effect transducer. Since EIS field-effect devices are capable for detection of any kind of charge changes at the gate insulator–electrolyte interface induced by molecular interactions or (bio-)chemical reactions, in the future, the realization of a large class of EIS-based chemical and biomolecular single logic gates and even an array of concatenated logic gates could be possible by applying this transducer principle.

3 Polyelectrolyte-Modified EIS Sensors

3.1 *Label-Free Detection of DNA with PAH-Modified EIS Sensor*

DNA biosensors and microarrays are considered as a powerful tool in many fields of applications ranging from pathogen identification and diagnosis of genetic diseases over drug and food industry to forensic testing or detection of biowarfare agents [15, 69–72]. Most of the DNA detection techniques are based on a highly specific DNA hybridization reaction by which a single-stranded probe DNA (ssDNA) binds to a complementary single-stranded target DNA (cDNA), forming a double-stranded DNA (dsDNA) with a well-known helix structure. For a signal readout and sensitivity enhancement, these techniques often require labeling of either the target or probe DNA molecules using various markers (e.g., fluorescence, redox, enzymatic, radiochemical) that make them time-consuming, complicated, and expensive [69, 73]. For the creation of inexpensive and simple genosensors or DNA chips, label-free detection principles are preferred. Therefore, considerable research efforts have been invested toward the label-free electrical detection of DNA by its intrinsic molecular charge using various kinds of FEDs (see, e.g., recent reviews [15, 16, 24, 74]). Examples are detection of DNA immobilization, hybridization, and denaturation [25, 75, 76], identification of single nucleotide polymorphism [77], monitoring of DNA extension reaction and sequencing [78, 79], as well as verification of DNA amplification by polymerase chain reaction (PCR) [80, 81]. In these devices, the binding/adsorption of negatively charged DNA molecules on the gate surface of the FED effectively changes the charge applied to the gate, resulting in a modulation of the flat band or threshold voltage and the output signal of the FED.

The major disadvantage of electrostatic DNA detection is the screening of the negative charge of DNA molecules by mobile ions in the surrounding solution that could significantly reduce the sensor signal, especially in high ionic strength solutions. FEDs are able to detect the charge changes that occur directly at the gate surface or within the order of the Debye screening length from the surface. The Debye length defines the distance at which the electrostatic potential drops $1/e$; it is inversely proportional to the ionic strength of the solution and amounts to be, for instance, ~ 1 nm for a 0.1 M solution of monovalent 1:1 salt. As a consequence, the electrostatic coupling between the charged DNA molecule and the FED strongly depends on the ionic strength of the solution, the distance between the charge of the molecule and the gate surface, and, therefore, on the orientation of DNA molecules to the gate surface. For example, if the DNA molecules are tethered to the gate surface via linker molecules or a spacer, the fraction of DNA charge that remains in the double layer and, thus, the FED signal induced by the DNA hybridization will strongly drop with increasing length of linker molecules. These problems can be overcome by immobilizing DNA molecules flat to the FED surface as well as by signal readout in a low ionic strength solution.

Direct electrostatic adsorption of DNA molecules onto typically used gate insulator (e.g., SiO_2 , Ta_2O_5 , Si_3N_4) surfaces is, in general, impossible, because both are negatively charged in a wide pH range. Therefore, recently, we proposed a strategy for the electrostatic detection of ssDNA adsorption and subsequent DNA hybridization on the gate surface of an EIS sensor modified with a positively charged weak polyelectrolyte layer of PAH [82–84]. Generally, a modification of the sensor surface by means of LbL electrostatic adsorption of a cationic polyelectrolyte/DNA bilayer becomes more popular in DNA biosensor design based on the field-effect platform [85, 86]. It has been discussed that in the presence of a positively charged polyelectrolyte layer, the electrostatically adsorbed DNA molecules will form preferentially flat-oriented elongated structures on the sensor surface with the molecular charges positioned near the gate surface within the Debye length, yielding a higher detection signal [82, 83]. Moreover, in contrast to often applied covalent immobilization methods that require time-consuming, cost-intensive procedures and complicated chemistry for functionalization of the gate surface and/or DNA molecules, the LbL adsorption technique is easy, fast, and cost-effective.

In the following, we present results of an application of PAH-modified Al–p-Si– SiO_2 EIS sensors for the label-free detection of a so-called on-chip and in-solution hybridization of DNA molecules, schematically shown in Fig. 7. In case of the on-chip hybridization, probe ssDNA molecules of known sequences were immobilized onto the PAH-modified FED surface, and the subsequent hybridization event was either detected in-situ by monitoring the sensor signal during the hybridization process or ex-situ by measuring the sensor signal before and after hybridization reaction. In contrast, by in-solution hybridization, the EIS sensor directly detects the electrostatic adsorption of dsDNA molecules formed after hybridization reaction occurred in the solution. In some cases, this could offer several advantages over detection by on-chip hybridization, especially, when the field-effect sensor is used for the detection of DNA amplification by PCR [80, 81]. By direct dsDNA detection, the surface modification procedure can be significantly simplified, because no probe ssDNA molecules have to be immobilized onto the sensor surface that could reduce both the detection time and costs.

Figure 7 demonstrates an example of detection of on-chip (a) and in-solution (b) hybridized DNA molecules with PAH-modified EIS sensors. In this experiment, the ConCap response has been recorded before and after each surface modification step: PAH adsorption, probe ssDNA immobilization on the PAH layer, and subsequent hybridization with complementary target cDNA as well as dsDNA adsorption on the PAH layer. The PAH layer (with thickness of about 2 nm) was prepared by exposing the Al–p-Si– SiO_2 EIS sensor to 50 μM PAH solution (pH 5.4) for 10 min. As it has been discussed in [82], at pH 5.4, both the SiO_2 surface and PAH molecules can be considered to be sufficiently charged to provide a successful electrostatic adsorption of positively charged PAH molecules onto the negatively charged SiO_2 surface. For probe ssDNA immobilization, the PAH-modified chip surface was exposed to 5 μM ssDNA solution for 1 h. For hybridization, the chip

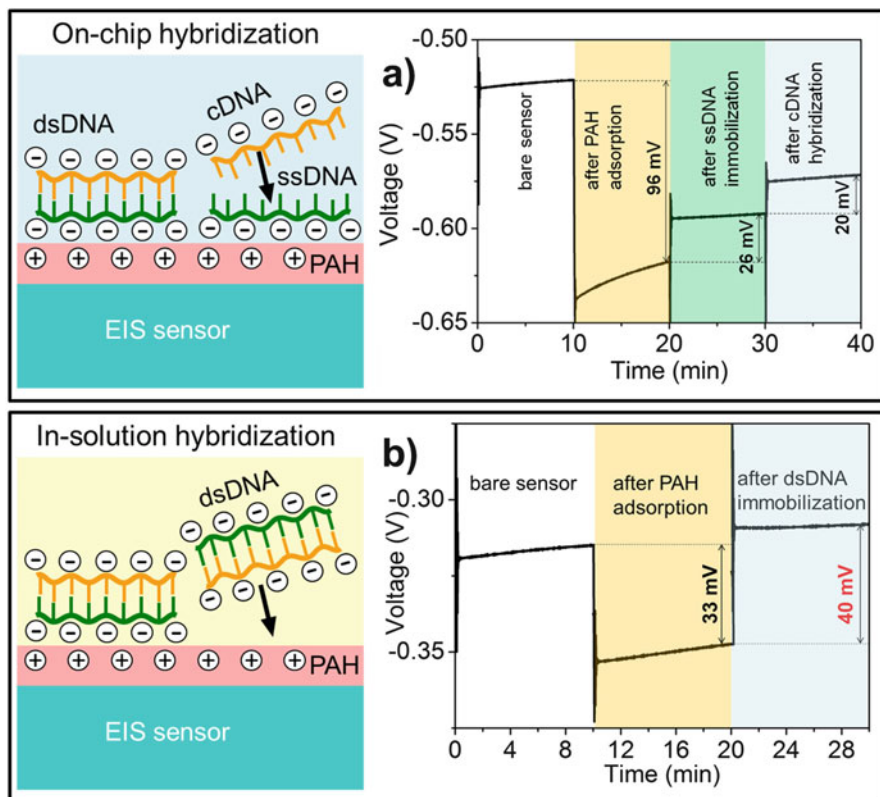


Fig. 7 Label-free detection of an on-chip (a) and in-solution (b) hybridization of 40-mer probe ssDNA with 20-mer cDNA molecules. To reduce the charge-screening effect and, thus, to enhance the sensitivity of the EIS sensor to the molecular charge, all measurements were performed in a low ionic strength solution (0.33 mM PBS buffer, pH 7, 5 mM NaCl)

surface covered with the PAH/ssDNA bilayer was incubated with target cDNA solution (5 μM cDNA) for 40 min at room temperature. For dsDNA adsorption, the PAH-modified SiO_2 surface was exposed to a solution containing in-solution hybridized dsDNA molecules for 1 h. The in-solution hybridization was achieved by mixing the solutions containing 5 μM probe ssDNA (40-mer) and 5 μM complementary target cDNA (20-mer) for 1 h. For the experimental details, see [82–84].

The consecutive adsorption of oppositely charged PAH and probe ssDNA layers leads to alternating potential shifts of about 96 and 26 mV, respectively (Fig. 7a). As it has been discussed in Sect. 2.2, the direction of these potential shifts depends on the sign of the charge of the adsorbed outermost layer, while the amplitude reflects the amount of adsorbed charge. If a positively charged PAH layer is adsorbed onto the negatively charged SiO_2 surface, one needs to apply a more negative gate voltage to compensate for this positive charge and to keep the capacitance constant. In contrast, the adsorption of negatively charged probe

ssDNA molecules shifts the sensor signal toward the direction of more positive (or less negative) bias voltages. After the hybridization process, the negative charge of the dsDNA molecules is increased, resulting in an additional potential shift (hybridization signal) of 20 mV in the direction of less negative voltages.

The average potential shift of about 40 mV was achieved after the adsorption of in-solution hybridized dsDNA molecules onto the PAH-modified EIS sensor surface (Fig. 7b). The lower detection limit evaluated from measurements in LAPS setup [84] was ~ 0.1 nM dsDNA that is in good agreement with results reported previously for DNA sensors based on silicon nanowires [87]. It is worth to note that the PAH-modified EIS-based DNA sensors, generally, exhibited better operating characteristics than EIS sensors modified with poly-L-lysine layer reported in [26].

3.2 Biosensors Based on an EIS Sensor Modified with a PAH/Enzyme Multilayer

At present, a lot of field-effect enzyme biosensors for the detection of various analytes (glucose, lactose, creatinine, penicillin, urea, organophosphorus pesticides, etc.) have been developed using different immobilization methods (see, e.g., [13, 88, 89]). These include, for instance, physical adsorption, covalent binding, cross-linking, entrapment within polymeric membranes, etc. The working characteristics (sensitivity, detection limit, response time, lifetime) of enzyme biosensors are strongly affected by the method of enzyme immobilization onto the transducer surface. With the aim to enhance biosensor performance, a completely different enzyme immobilization strategy has been proposed in [90], which is based on a modification of the EIS sensor surface with a pH-responsive weak PE/enzyme multilayer. Such modified EIS biosensor is capable for sensing not only local pH changes on the gate surface induced by the enzymatic reaction but also pH-induced changes in the charge of the weak PE macromolecules. In the following, the proposed concept is described in detail, taking the example of a penicillin biosensor prepared via modification of a SiO₂ gate EIS structure with a PAH/penicillinase multilayer (see Fig. 8).

The working principle of the field-effect penicillin biosensor is based on the detection of H⁺ ions, which are produced during the hydrolysis of penicillin catalyzed by the enzyme penicillinase [91]. The resulting local pH decrease near the surface of the gate insulator (here, SiO₂) will change the surface charge of the SiO₂ and, thus, will shift the $C-V$ curve of the field-effect sensor along the voltage axis (see, Fig. 8). The magnitude of this shift (ΔV_s) depends on the local pH change (ΔpH) and, therefore, on the penicillin concentration in the solution. On the other hand, if the enzyme penicillinase is embedded within the multilayer of a weak PE of PAH exhibiting pH-responsive ionizable groups [92], the local pH changes induced by the enzymatic reaction will also alter the effective molecular charge of the polyelectrolyte and charge density within the multilayer. This will cause an

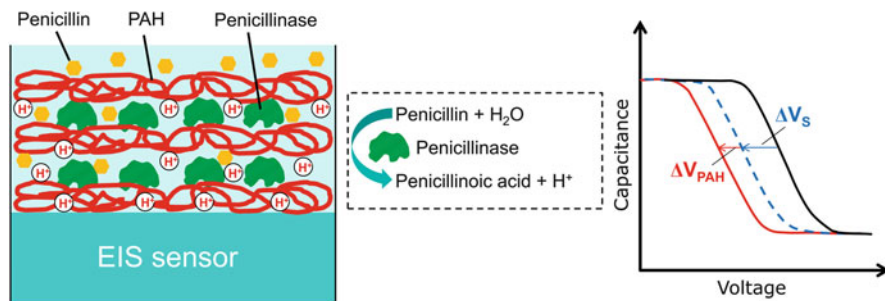


Fig. 8 Functioning principle of a penicillin-sensitive EIS biosensor modified with a pH-responsive weak PE/enzyme multilayer: schematic structure (*left*); enzymatic reaction of catalyzed hydrolysis of penicillin by the enzyme penicillinase (*middle*); expected shift of the C - V curves of the EIS sensor (*right*)

additional shift of the C - V curve along the voltage axis (ΔV_{PAH}). Consequently, for the EIS sensor modified with a weak PE/enzyme multilayer, a large sensor signal and a higher sensitivity should be expected.

In order to prove the described detection mechanism, the pH and penicillin sensitivity of an $Al-p-Si-SiO_2-(PAH/penicillinase)_3-PAH$ structure with LbL-prepared three bilayers of PAH/penicillinase and PAH as outermost layer has been studied [90]. For comparison, penicillin sensitivity of an $Al-p-Si-SiO_2$ -penicillinase structure with adsorptively immobilized penicillinase has been tested, too. The pH sensitivity of the EIS sensor modified with the PAH/penicillinase multilayer was higher (52 mV/pH in the range from pH 5 to 8) than that of a bare SiO_2 gate EIS sensor (38 mV/pH). As it has been reported in [92, 93], the ionization degree and, therefore, the molecular charge of weak PE in the embedded layer changes with both the pH of the surrounding solution and the net charge of the outermost layer. Thus, the higher pH sensitivity of the modified EIS sensor can be explained by assuming that both the underlying SiO_2 gate insulator and the effective molecular charge of the PAH multilayer contribute to the pH-dependent sensor response.

As expected, the higher penicillin sensitivity (around 100 mV/decade in the linear range of 0.25–2.5 mM penicillin G) has been obtained for the $Al-p-Si-SiO_2-(PAH/penicillinase)_3-PAH$ sensor (for comparison, penicillin sensitivity of the $Al-p-Si-SiO_2$ sensor with adsorptively immobilized penicillinase was ~ 45 mV/decade [90, 91]). The lower and upper detection limit was around 0.02 and 10 mM, respectively. The 90% response time was about 1 min. Long-term measurements show that even after 2 months, the loss of the original penicillin sensitivity was only around 10–12% [90].

Taking together, an incorporation of enzymes in a weak PE multilayer provides high analyte sensitivity, reduces enzyme leaching effects, and, thus, enhances the operation stability and lifetime of the biosensor. Moreover, an entrapment of enzymes within a polyelectrolyte multilayer could provide a larger amount of

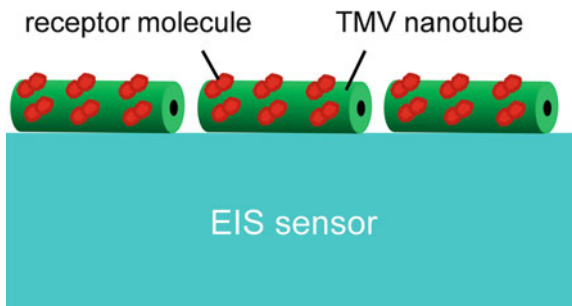
enzymes immobilized per sensor area [90]. Finally, the described strategy could be extended to further enzyme-based field-effect biosensors.

4 Summary and Outlook

During the last few years, label-free biosensing has become one of the most reported research fields for nanomaterial-modified capacitive EIS sensors. In this chapter, we presented selected examples of recent developments on EIS sensors modified with ligand-stabilized AuNPs or a weak PE layer for the electrostatic detection of charged molecules. The AuNP-modified EIS sensor detects charge changes in AuNP/ligand inorganic/organic hybrids induced by molecular adsorption or binding events. Since the vast majority of biomolecules are charged under physiological conditions and because the surface of AuNPs can be easily modified with different charged (positively/negatively) shell molecules, AuNP-modified EIS sensors represent a powerful and universal platform for label-free electrical detection of a wide variety of biomolecules by their intrinsic molecular charge. The feasibility of this approach has been demonstrated on examples of EIS sensors modified with citrate-stabilized negatively charged AuNPs for the electrostatic detection of positively charged CytC and PDL, representing typical model examples of detecting small proteins and PE macromolecules. In addition, AuNP-modified EIS sensors were successfully applied for the monitoring of a LbL buildup of PE multilayers of PAH/PSS as well as for the realization of enzyme logic gates. Furthermore, a label-free DNA sensor and enzyme-based biosensor with enhanced performance have been realized using EIS structures modified with a weak PE of PAH.

The presented approach can be extended to other FEDs as well as other charged molecules and even biological entities, e.g., virus particles. Nowadays, viruses are considered not only as disease-causing agents but also as highly promising smart materials for bio- and nanotechnology applications [94] as well as for biosensing [95]. The *tobacco mosaic virus* (TMV) is one of the most extensively studied plant viruses [94], which is nonpathogenic for mammals. TMV particles have a tubelike shape (with a typical length of about 300 nm, an outer diameter of 18 nm, and an inner channel diameter of 4 nm). The outer surface of the TMV nanotubes possesses thousands of regularly spaced sites that can be used for selective binding of molecules (see Fig. 9). For instance, recently, we successfully applied TMV nanotubes as enzyme nanocarriers for the development of an amperometric glucose biosensor [96]. The presence of TMV nanotubes on the sensor surface allows binding of a high amount of precisely positioned enzymes without substantial loss of their activity and may also ensure accessibility of their active centers for analyte molecules. We believe that the integration of virus particles, in particular TMV nanotubes with FEDs (Fig. 9), will open new strategies in advanced label-free biosensing technology.

Fig. 9 Schematic of the EIS sensor modified with TMV nanotubes functionalized with receptor molecules



It is worth mentioning that in spite of successful experiments with nanomaterial-modified FEDs, the label-free electrostatic detection of charged biomolecules in real samples, especially in biological samples such as blood, urine, or saliva, remains still a major challenge. Biological samples are very complex mixtures of proteins, ions, and other chemical species. A possible nonspecific adsorption of proteins and other charged molecules onto the sensor surface could generate false background signals in addition to the signals from analytes of interest. Therefore, reduction of nonspecific adsorption of biomolecules is evident in label-free biosensor development and commercialization. Various blocking agents, like bovine serum albumin or polyethylene glycol, have been used to reduce nonspecific adsorption on biosensor surfaces. The problem of nonspecific response can also be reduced by pre-filtering/purifying the complex biological liquids or by applying differential-mode measurements.

Acknowledgments The authors thank M. Bäcker, D. Mayer, M. Weil, and E. Katz for valuable discussion and H. Iken, T.S. Bronder, S. Scheja, P. Mehndiratta, and M. Jablonski for technical support.

References

1. Noguchi Y, Yamamoto M, Ishii H, Ueda R, Terui T, Imazu K, Tamada K, Sakano T, Matsuda K (2013) Photoresponses in gold nanoparticle single-electron transistors with molecular floating gates. *Jpn J Appl Phys* 52:110102
2. Khondaker SI, Luo K, Yao Z (2010) The fabrication of single-electron transistors using dielectrophoretic trapping of individual gold nanoparticles. *Nanotechnology* 21:095204
3. Diez-Perez I, Li Z, Guo S, Madden C, Huang H, Che Y, Yang X, Zang L, Tao N (2012) Ambipolar transport in an electrochemically gated single-molecule field-effect transistor. *ACS Nano* 6:7044–7052
4. Chen YS, Hong MY, Huang GS (2012) A protein transistor made of an antibody molecule and two gold nanoparticles. *Nat Nanotechnol* 7:197–203
5. Poghossian A, Bäcker M, Mayer D, Schöning MJ (2015) Gating capacitive field-effect sensors by the charge of nanoparticle/molecule hybrids. *Nanoscale* 7:1023–1031
6. Samanta A, Medintz IL (2016) Nanoparticles and DNA – a powerful and growing functional combination in bionanotechnology. *Nanoscale* 8:9037–9095

7. Willner I, Baron R, Willner B (2007) Integrated nanoparticle-biomolecule systems for biosensing and bioelectronics. *Biosens Bioelectron* 22:1841–1852
8. Mehrabani S, Maker AJ, Armani AM (2014) Hybrid integrated label-free chemical and biological sensors. *Sensors* 14:5890–5928
9. Boettcher SW, Strandwitz NC, Schierhorn M, Lock N, Lonergan MC, Stucky GD (2007) Tunable electronic interfaces between bulk semiconductors and ligand-stabilised inorganic nanoparticle assemblies. *Nat Mater* 6:592–596
10. Gun J, Gutkin V, Lev O, Boyen HG, Saitner M, Wagner P, D’Olieslaeger M, Abouzar MH, Poghossian A, Schöning MJ (2011) Tracing gold nanoparticle charge by electrolyte-insulator-semiconductor devices. *J Phys Chem C* 115:4439–4445
11. Siqueira Jr JR, Abouzar MH, Bäcker M, Zucolotto V, Poghossian A, Oliveira Jr ON, Schöning MJ (2009) Carbon nanotubes in nanostructured films: potential application as amperometric and potentiometric field-effect (bio-)chemical sensors. *Phys Status Solidi A* 206:462–467
12. Jimenez-Jorquera C, Orozco J, Baldi A (2010) ISFET based microsensors for environmental monitoring. *Sensors* 10:61–83
13. Lee CS, Kim SK, Kim M (2009) Ion-sensitive field-effect transistor for biological sensing. *Sensors* 9:7111–7131
14. Nakazato K (2009) An integrated ISFET sensor array. *Sensors* 9:8831–8851
15. Poghossian A, Schöning MJ (2014) Label-free sensing of biomolecules with field-effect devices for clinical applications. *Electroanalysis* 26:1197–1213
16. Pachauri V, Ingebrandt S (2016) Biologically sensitive field-effect transistors: from ISFETs to NanoFETs. *Essays Biochem* 60:81–90
17. Zhou W, Dai X, Lieber CM (2017) Advances in nanowire bioelectronics. *Rep Prog Phys* 80:016701
18. Zhang A, Lieber CM (2016) Nano-bioelectronics. *Chem Rev* 116:215–257
19. Rolka D, Poghossian A, Schöning MJ (2004) Integration of a capacitive EIS sensor into a FIA system for pH and penicillin determination. *Sensors* 4:84–94
20. Gun J, Rizkov D, Lev O, Abouzar MH, Poghossian A, Schöning MJ (2009) Oxygen plasma-treated gold nanoparticle-based field-effect devices as transducer structures for (bio-)chemical sensing. *Microchim Acta* 164:395–404
21. Beyer M, Menzel C, Quack R, Scheper T, Schügerl K, Treichel W, Voigt H, Ullrich M, Ferretti R (1994) Development and application of a new enzyme sensor type based on the EIS capacitance structure for bioprocess control. *Biosens Bioelectron* 9:17–21
22. Menzel C, Lerch T, Scheper T, Schügerl K (1995) Development of biosensors based on an electrolyte insulator semiconductor (EIS) capacitor structure and their application for process monitoring. *Anal Chim Acta* 317:259–264
23. Poghossian A, Ingebrandt S, Abouzar MH, Schöning MJ (2007) Label-free detection of charged macromolecules by using a field-effect-based sensor platform: experiments and possible mechanisms of signal generation. *Appl Phys A Mater Sci Process* 87:517–524
24. Kataoka-Hamai C, Miyahara Y (2011) Label-free detection of DNA by field-effect devices. *IEEE Sensors J* 11:3153–3160
25. Abouzar MH, Poghossian A, Cherstvy AG, Pedraza AM, Ingebrandt S, Schöning MJ (2012) Label-free electrical detection of DNA by means of field-effect nanoplate capacitors: experiments and modeling. *Phys Status Solidi A* 209:925–934
26. Hou CSJ, Milovic N, Godin M, Russo PR, Chakrabarti R, Manalis SR (2006) Label-free microelectronic PCR quantification. *Anal Chem* 78:2526–2531
27. Tiwari PM, Vig K, Dennis VA, Singh SR (2011) Functionalized gold nanoparticles and their biomedical applications. *Nano* 1:31–63
28. Pelaz B, Jaber S, Jimenez de Aberasturi D, Wulf V, Aida T, de la Fuente JM, Feldmann J, Gaub JHE, Josephson L, Kagan CR, Kotov NA, Liz-Marzán LM, Mattoussi H, Mulvaney P, Murray CB, Rogach AL, Weiss PS, Willner I, Parak W (2012) The state of nanoparticle-based nanoscience and biotechnology: progress, promises, and challenges. *ACS Nano* 6:8468–8483

29. Zabet-Khosousi A, Dhirani A (2008) Charge transport in nanoparticle assemblies. *Chem Rev* 108:4072–4124
30. Luo X, Morrin A, Killard AJ, Smyth MR (2006) Application of nanoparticles in electrochemical sensors and biosensors. *Electroanalysis* 18:319–326
31. Giljohann DA, Seferos DS, Daniel WL, Massich MD, Patel PC, Mirkin CA (2010) Gold nanoparticles for biology and medicine. *Angew Chem Int Ed* 49:3280–3294
32. Yeh YC, Creran B, Rotello VM (2012) Gold nanoparticles: preparation, properties, and applications in bionanotechnology. *Nanoscale* 4:1871–1880
33. Gun J, Schöning MJ, Abouzar MH, Poghossian A, Katz E (2008) Field-effect nanoparticle-based glucose sensor on a chip: amplification effect of coimmobilized redox species. *Electroanalysis* 20:1748–1753
34. Pita M, Krämer M, Zhou J, Poghossian A, Schöning MJ, Fernandez VM, Katz E (2008) Optoelectronic properties of nanostructured ensembles controlled by biomolecular logic systems. *ACS Nano* 2:2160–2166
35. Krämer M, Pita M, Zhou J, Ornatska M, Poghossian A, Schöning MJ, Katz E (2009) Coupling of biocomputing systems with electronic chips: electronic interface for transduction of biochemical information. *J Phys Chem C* 113:2573–2579
36. Ghosh P, Han G, De M, Kim CK, Rotello VM (2008) Gold nanoparticles in delivery applications. *Adv Drug Deliv Rev* 60:1307–1315
37. Fu Y, Yuan R, Xu L, Chai Y, Zhong X, Tang D (2005) Indicator-free DNA hybridization detection via EIS based on self-assembled gold nanoparticles and bilayer two-dimensional 3-mercaptopropyltrimethoxysilane onto a gold substrate. *Biochem Eng J* 23:37–44
38. Kruglenko I, Shirshov Y, Burlachenko J, Savchenko A, Kukla O, Belyaev O (2012) Sensor for detection of water presence in gaseous mixtures based on gold nanoparticles stabilized by sodium citrate. *Sensors Actuators B Chem* 170:109–114
39. Polavarapu L, Xu QH (2009) A simple method for large scale synthesis of highly monodisperse gold nanoparticles at room temperature and their electron relaxation properties. *Nanotechnology* 20:185606
40. Poghossian A, Weil M, Cherstvy AG, Schöning MJ (2013) Electrical monitoring of polyelectrolyte multilayer formation by means of capacitive field-effect devices. *Anal Bioanal Chem* 405:6425–6436
41. Bergveld P (1991) A critical evaluation of direct electrical protein detection methods. *Biosens Bioelectron* 6:55–72
42. Vinu A, Murugesan V, Tangermann O, Hartmann M (2004) Adsorption of cytochrome c on mesoporous molecular sieves: influence of pH, pore diameter, and aluminum incorporation. *Chem Mater* 16:3056–3065
43. Bonk SM, Lisdat F (2009) Layer-by-layer assembly of electro-active gold nanoparticle/cytochrome c multilayers. *Biosens Bioelectron* 25:739–744
44. Imabayashi S, Mita T, Kakiuchi T (2005) Effect of the electrostatic interaction on the redox reaction of positively charged cytochrome c adsorbed on the negatively charged surfaces of acid-terminated alkanethiol monolayers on a Au(111) electrode. *Langmuir* 21:1470–1474
45. Stobiecka M, Hepel M (2011) Double-shell gold nanoparticle-based DNA carriers with poly-L-lysine binding surface. *Biomaterials* 32:3312–3321
46. Murthy VS, Cha JN, Stucky GD, Wong MS (2004) Charge-driven flocculation of poly(L-lysine)-gold nanoparticle assemblies leading to hollow microspheres. *J Am Chem Soc* 126:5292–5299
47. Decher G, Eckle M, Schmitt J, Struth B (1998) Layer-by-layer assembled multicomposite films. *Curr Opin Colloid Interface Sci* 3:32–39
48. Schönhoff M, Ball V, Bausch AR, Dejugnat C, Delorme N, Glinel K, Klitzing R, Steitz R (2007) Hydration and internal properties of polyelectrolyte multilayers. *Colloids Surf A Physicochem Eng Asp* 303:14–29

49. Abouzar MH, Poghossian A, Pedraza AM, Gandhi D, Ingebrandt S, Moritz W, Schöning MJ (2011) An array of field-effect nanoplate SOI capacitors for (bio-)chemical sensing. *Biosens Bioelectron* 26:3023–3028
50. Garyfallou GZ, de Smet LCPM, Sudhölter EJR (2012) Characteristics of electrolyte-oxide-silicon sensors: pH sensing and polyelectrolyte adsorption. *Sensors Actuators B Chem* 168:207–213
51. Neff PA, Wunderlich BK, Klitzing R, Bausch AR (2007) Formation and dielectric properties of polyelectrolyte multilayers studied by a silicon-on-insulator based thin film resistor. *Langmuir* 23:4048–4052
52. Poghossian A, Abouzar MH, Sakkari M, Kassab T, Han Y, Ingebrandt S, Offenhäuser A, Schöning MJ (2006) Field-effect sensors for monitoring the layer-by-layer adsorption of charged macromolecules. *Sensors Actuators B Chem* 11:163–170
53. Vu XT, Stockmann R, Wolfrum B, Offenhäuser A, Ingebrandt S (2010) Fabrication and application of a microfluidic-embedded silicon nanowire biosensor chip. *Phys Status Solidi A* 207:850–857
54. Gorin DA, Yashchenok AM, Manturov AO, Kolesnikova TA, Möhwald H (2009) Effect of layer-by-layer electrostatic assemblies on the surface potential and current voltage characteristic of metal–insulator–semiconductor structures. *Langmuir* 25:12529–12534
55. Smith RN, McCormick M, Barrett CJ, Reven L, Spiess HW (2004) NMR studies of PAH/PSS polyelectrolyte multilayers adsorbed onto silica. *Macromolecules* 37:4830–4838
56. Andreasson J, Pischel U (2015) Molecules with a sense of logic: a progress report. *Chem Soc Rev* 44:1053–1069
57. Pischel U, Andreasson J, Gust D, Pais VF (2013) Information processing with molecules – quovadis? *ChemPhysChem* 14:28–46
58. Katz E, Privman V (2010) Enzyme-based logic systems for information processing. *Chem Soc Rev* 39:1835–1857
59. Wang J, Katz E (2010) Digital biosensors with built-in logic for biomedical applications – biosensors based on a biocomputing concept. *Anal Bioanal Chem* 398:1591–1603
60. Katz E, Poghossian A, Schöning MJ (2017) Enzyme-based logic gates and circuits – analytical applications and interfacing with electronics. *Anal Bioanal Chem* 409:81–94
61. Lai YH, Sun SC, Chuang MC (2014) Biosensors with built-in biomolecular logic gates for practical applications. *Biosensors* 4:273–300
62. Poghossian A, Malzahn K, Abouzar MH, Mehndiratta P, Katz E, Schöning MJ (2011) Integration of biomolecular logic gates with field-effect transducers. *Electrochim Acta* 56:9661–9665
63. Molinnus D, Sorich M, Bartz A, Siegert P, Willenberg HS, Lisdat F, Poghossian A, Keusgen M, Schöning MJ (2016) Towards an adrenaline biosensor based on substrate recycling amplification in combination with an enzyme logic gate. *Sensors Actuators B Chem* 237:190–195
64. Liu J, Zhou H, Xu JJ, Chen HY (2013) Dual-biomarker-based logic-controlled electrochemical diagnosis for prostate cancers. *Electrochem Commun* 32:27–30
65. Katz E, Minko S (2015) Enzyme-based logic systems interfaced with signal-responsive materials and electrodes. *Chem Commun* 51:3493–3500
66. Molinnus D, Bäcker M, Iken H, Poghossian A, Keusgen M, Schöning MJ (2015) Concept for a biomolecular logic chip with an integrated sensor and actuator function. *Phys Status Solidi A* 212:1382–1388
67. Poghossian A, Katz E, Schöning MJ (2015) Enzyme logic AND-Reset and OR-Reset gates based on a field-effect electronic transducer modified with multi-enzyme membrane. *Chem Commun* 51:6564–6567
68. Cane C, Gracia I, Merlos A (1997) Microtechnologies for pH ISFET chemical sensors. *Microelectron J* 28:389–405
69. Sassolas A, Leca-Bouvier BD, Blum LJ (2008) DNA biosensors and microarrays. *Chem Rev* 108:109–139

70. Wei F, Lillehoj PB, Ho CM (2010) DNA diagnostics: nanotechnology-enhanced electrochemical detection of nucleic acids. *Pediatr Res* 67:458–468
71. Choi S, Goryll M, Sin LYM, Wong PK, Chae J (2011) Microfluidic-based biosensors toward point-of-care detection of nucleic acids and proteins. *Microfluid Nanofluid* 10:231–247
72. Palecek E, Bartosik M (2012) Electrochemistry of nucleic acids. *Chem Rev* 112:3427–3481
73. Javanmard M, Davis RW (2011) A microfluidic platform for electrical detection of DNA hybridization. *Sensors Actuators B Chem* 154:22–27
74. Veigas B, Fortunato E, Baptista PV (2015) Field effect sensors for nucleic acid detection: recent advances and future perspectives. *Sensors* 15:10380–10398
75. Wu C, Bronder T, Poghossian A, Werner CF, Bäcker M, Schöning MJ (2014) Label-free electrical detection of DNA with a multi-spot LAPS: first step towards light-addressable DNA chips. *Phys Status Solidi A* 211:1423–1428
76. Lu N, Gao A, Dai P, Li T, Wang Y, Gao X, Song S, Fan C, Wang Y (2013) Ultra-sensitive nucleic acids detection with electrical nanosensors based on CMOS-compatible silicon nanowire field-effect transistors. *Methods* 63:212–218
77. Ingebrandt S, Han Y, Nakamura F, Poghossian A, Schöning MJ, Offenhäusser A (2007) Label-free detection of single nucleotide polymorphisms utilizing the differential transfer function of field-effect transistors. *Biosens Bioelectron* 22:2834–2840
78. Kamahori M, Ishige Y, Shimoda M (2008) Detection of DNA hybridization and extension reactions by an extended-gate field-effect transistor: characterizations of immobilized DNA-probes and role of applying a superimposed high-frequency voltage onto a reference electrode. *Biosens Bioelectron* 23:1046–1054
79. Sakata T, Miyahara Y (2006) DNA sequencing based on intrinsic molecular charges. *Angew Chem Int Ed* 45:2225–2228
80. Hou CSJ, Godin M, Payer K, Chakrabarti R, Manalis SR (2007) Integrated microelectronic device for label-free nucleic acid amplification and detection. *Lab Chip* 7:347–354
81. Veigas B, Branquinho R, Pinto JV, Wojcik PJ, Martins R, Fortunato E, Baptista PV (2014) Ion sensing (EIS) real-time quantitative monitorization of isothermal DNA amplification. *Biosens Bioelectron* 52:50–55
82. CS W, Bronder T, Poghossian A, Werner CF, Schöning MJ (2015) Label-free detection of DNA using a light-addressable potentiometric sensor modified with a positively charged polyelectrolyte layer. *Nanoscale* 7:6143–6150
83. Bronder TS, Poghossian A, Scheja S, Wu C, Keusgen M, Mewes D, Schöning MJ (2015) DNA immobilization and hybridization detection by the intrinsic molecular charge using capacitive field-effect sensors modified with a charged weak polyelectrolyte layer. *ACS Appl Mater Interfaces* 7:20068–20075
84. Wu C, Poghossian A, Bronder TS, Schöning MJ (2016) Sensing of double-stranded DNA molecules by their intrinsic molecular charge using the light-addressable potentiometric sensor. *Sensors Actuators B Chem* 229:506–512
85. Braeken D, Reekmans G, Zhou C, van Meerbergen B, Callewaert G, Borghs G, Bartic C (2008) Electronic DNA hybridisation detection in low-ionic strength solutions. *J Exp Nanosci* 3:157–169
86. Wang J, Zhou YL, Watkinson M, Gautrot J, Krause S (2015) High-sensitivity light-addressable potentiometric sensors using silicon on sapphire functionalized with self-assembled organic monolayers. *Sensors Actuators B Chem* 209:230–236
87. Adam T, Hashim U (2015) Highly sensitive silicon nanowire biosensor with novel liquid gate control for detection of specific single-stranded DNA molecules. *Biosens Bioelectron* 67:656–661
88. Dzyadevych SV, Soldatkin AP, El'skaya AV, Martelet C, Jaffrezic-Renault N (2006) Enzyme biosensors based on ion-selective field-effect transistors. *Anal Chim Acta* 568:248–258
89. Schöning MJ, Poghossian A (2006) Bio FEDs (field-effect devices): state-of-the-art and new directions. *Electroanalysis* 18:1893–1900

90. Abouzar MH, Poghossian A, Siqueira Jr JR, Oliveira Jr ON, Moritz W, Schöning MJ (2010) Capacitive electrolyte–insulator–semiconductor structures functionalised with a polyelectrolyte/enzyme multilayer: new strategy for enhanced field-effect biosensing. *Phys Status Solidi A* 207:884–890
91. Beging S, Leinhos M, Jablonski M, Poghossian A, Schöning MJ (2015) Studying the spatially resolved immobilisation of enzymes on a capacitive field-effect structure by means of nanospotting. *Phys Status Solidi A* 212:1353–1358
92. Mauser T, Dejugnat C, Sukhorukov GB (2004) Reversible pH-dependent properties of multilayer microcapsules made of weak polyelectrolytes. *Macromol Rapid Commun* 25:1781–1785
93. Xie AF, Gramick S (2002) Local electrostatics within a polyelectrolyte multilayer with embedded weak polyelectrolyte. *Macromolecules* 35:1805–1813
94. Culver JN, Brown AD, Zang F, Gnerlich M, Gerasopoulos K, Ghodssi R (2015) Plant virus directed fabrication of nanoscale materials and devices. *Virology* 479–480:200–212
95. Fan XZ, Pomerantseva E, Gnerlich M, Brown AD, Gerasopoulos K, McCarthy M, Culver JN, Ghodssi R (2013) Tobacco mosaic virus: a biological building block for micro/nano/bio systems. *J Vac Sci Technol A* 31:050815
96. Bäcker M, Koch C, Eiben S, Geiger F, Eber F, Gliemann H, Poghossian A, Wege C, Schöning MJ (2016) Tobacco mosaic virus as enzyme nanocarrier for electrochemical biosensors. *Sensors Actuators B Chem* 238:716–722